

FINITE ELEMENT ANALYSIS OF BLOOD FLOW AND HEAT TRANSPORT IN THE HUMAN FINGER

**Ying He¹, Hao Liu², Ryutaro Himeno³,
Junko Sunaga⁴, Nobunori Kakusho⁵, and Hideo Yokota⁶**

¹ Computational Biomechanics Unit, RIKEN,
2-1 Hirosawa, Wako-shi, Saitama 351-0198, Japan
e-mail: heyings@riken.jp

² Faculty of Engineering, Chiba University,
1-33 Yayoi-cho, Inage-ku, Chiba 263-8522 Japan
hliu@faculty.chiba-u.ac.jp

³ Computational Biomechanics Unit, RIKEN,
2-1 Hirosawa, Wako-shi, Saitama 351-0198, Japan
himeno@riken.jp

⁴ Computational Biomechanics Unit, RIKEN,
2-1 Hirosawa, Wako-shi, Saitama 351-0198, Japan
j-sunaga@riken.jp

⁵ Computational Biomechanics Unit, RIKEN,
2-1 Hirosawa, Wako-shi, Saitama 351-0198, Japan
kakusho@riken.jp

⁶ Computational Biomechanics Unit, RIKEN,
2-1 Hirosawa, Wako-shi, Saitama 351-0198, Japan
hyokota@riken.jp

Abstract The human finger is said to be the extension of the brain and can convey the information on mechanical, thermal, and tissue damaging. The quantitative prediction of blood flow rate and thermal generation are of great importance for diagnosing blood circulation illness and for the noninvasive measurement of blood glucose. In this study, we developed a coupled thermofluid model to simulate blood flow in large vessels and living tissue. The finite element (FE) model to analyze the blood perfusion and heat transport in the human finger was developed based on the transport theory in porous media. With regard to the blood flow in the large arteries and veins, the systemic blood circulation in the upper limb was modeled based on the one-dimensional flow in an elastic tube. The blood pressure and velocity in each vessel were first computed and the corresponding values for the large vessels in the finger were subsequently transferred to the FE model as the boundary conditions. The realistic geometric model for the human finger was constructed based on the MRI image data. After computing the capillary pressure and blood velocity in the tissue, the temperatures in the large vessels and the tissue of the finger were computed simultaneously by numerically solving the energy equation in porous media. The computed results are in favorable agreement with the available data. It is believed that this analysis model will have extensive applications in the prediction of peripheral blood flow, temperature variation, and mass transport.

Key Words: Porous Media, Blood Perfusion, Finite Element Method, One-dimensional Blood Flow, Human Finger, Image-based Model, MR images

1. Introduction

Blood circulation performs an important function—to carry oxygen to the tissues and to remove carbon dioxide and other metabolites from the tissues. Thus, blood circulation plays a crucial role in thermoregulation and mass transport. The quantitative prediction of the relationship between hemodynamics and heat and mass transfer is of great interest, because it is related to human thermal comfort, drug delivery, and noninvasive measurement.

Biological tissues contain blood and the surrounding materials where blood is perfused to tissues via capillary network. The energy transport in tissues includes conduction in tissues, convection between blood and tissues, perfusion through microvascular beds, and metabolic heat generation. Among these, the heat transfer between blood and tissues could be of the greatest importance. The Pennes [1] bioheat equation is the most common method that is available to describe blood perfusion in the tissue. However, this method cannot explain the convection between large vessels and tissues but can only explain the uniform perfusion of blood to tissues.

Further, in another method, the spatial variations in the arterial, venous, and tissue temperatures are considered, and it includes three equations that represent the heat transfer in arteries, veins, and tissues. This method was first presented by Keller and Seiler [2] and has been developed and used by many other researchers [3], [4], [5], [6], [7]. These models are frequently applied in describing the whole body thermal system.

Researchers also intend to analyze heat transfer in living tissues by modeling the detailed countercurrent microvascular network. Chen and Homes [8] presented a bioheat transfer model that accounts for the thermally significant blood vessels. They treated the blood vessels as two groups—large vessels and small vessels. Each vessel is treated separately in the former group, whereas all vessels are treated as a part of a continuum in the latter group. The thermal contributions of the small blood vessels were considered from the equilibration of blood temperature, convection of the flowing blood, and the small temperature fluctuations of the nearly equilibrated blood. Weinbaum and Jiji [9] proposed an alternative model that accounts for the thermal effect of the directionality of the blood vessels and the characteristic geometry of the blood vessel arrangement. The vascular structure in the periphery was treated individually rather than as continuum media in their three-layer model. Brink and Werner [10] presented a three-dimensional thermal and vascular model in which the convective heat exchange between the feeder vessels and tissue was computed by the values for the Nusselt number and the temperatures in and near individual vessels were predicted. The thermally significant vessels were treated individually according to their distribution characteristics in different tissue layers.

From these modeling studies, it is evident that investigation of the thermal effects of large blood vessels and small vessels is the most important aspect. However, due to the high density and complex arrangement of microvessels, little information about vascular geometry can be obtained and the applications of the vascular models are limited for small volumes of tissue. Thus, it is of great importance to develop an easy-to-use model for describing the blood flow in different sizes of vessels.

On the other hand, a blood-perfused biological tissue can be described as a porous media in which the fluid phase represents the blood and the surrounding tissue is represented by the solid phase. The theory of porous media for heat transfer in living tissues may be the most appropriate since it can describe the perfused blood with fewer assumptions as compared to other bioheat models. Wulff [11] first dealt with the living tissue as a porous medium and utilized the convective term, including the Darcy velocity, to replace the blood perfusion term

in the bioheat equation. Xuan and Roetzel [12] used the transport theory through porous media to model the tissue-blood system. The blood and tissue were considered to be in a non-equilibrium state and two energy equations were used to express heat transfer in the blood phase and solid phase. The advantage of this model is that it includes the exact blood perfusion in tissues, blood dispersion, and effective tissue conductivity and is considered to be appropriate for modeling a blood-perfused tissue. However, the flow in large blood vessels differs from the filtration flow through tissues and may be considered separately.

Mesh generation based on the realistic geometric model is also of significance in performing thermal analysis in the living tissue. Geometrical modeling and mesh generation based on medical images (CT or MR images) are widely used in biofluid mechanics and biomechanics analysis [13,14]. The conventional steps to construct a computational model are image processing, geometrical modeling, and mesh generation. Although the different techniques in medical imaging and computational simulation need to be integrated, this technique provides a rapid and valid method to model the thermofluid and mechanics problems in living tissues.

The purpose of this study is to model blood-tissue heat transfer according to the different characteristics of blood flow in large vessels and tissues. The systemic blood circulation in the upper limb has been modeled based on the one-dimensional flow in an elastic tube, and the finite element (FE) model based on the heat transport in porous media was developed to analyze the blood perfusion and heat transport in the human finger. Further, the realistic geometric model for the human finger was constructed on the basis of MR image data. After computing the capillary pressure and blood velocity in the tissue, the temperatures of the large vessels and the finger tissue were computed simultaneously by numerically solving the energy equation in the porous media.

2. Modeling blood flow dynamics and heat transfer in tissues

2.1 Blood flow dynamics

The blood flow in large vessels has been modeled to be a one-dimensional flow in an elastic tube, and the governing equations, including continuity and momentum, are expressed as

$$\frac{\partial A}{\partial t} + \frac{\partial q}{\partial x} = 0 \quad (1)$$

$$\frac{\partial q}{\partial t} + \frac{\partial}{\partial x} \left(\frac{q^2}{A} \right) + \frac{A}{\rho} \frac{\partial P}{\partial x} = - \frac{2\pi r}{\delta} \frac{q}{A} \quad (2)$$

where x is the distance from the heart, t is the time, A is the cross-sectional area of the blood vessel, q is the blood flow rate, P is the transmural pressure, ρ is the blood density, v is the kinematic viscosity, δ is the boundary-layer thickness, and r is the radius of the blood vessel. The pressure-area relationship for the arteries and veins is as follows:

$$P(x, t) - P_0 = \frac{4}{3} \frac{Eh}{r_0} \left(1 - \sqrt{\frac{A_0}{A}} \right) \quad (3)$$

$$p - p_0 = k_p \left[1 - \left(\frac{A}{A_0} \right)^{-3/2} \right] \quad (4)$$

where E is Young's modulus, h is the wall thickness of the blood vessel, and k_p is the coefficient that is proportional to the bending stiffness of the tube wall.

A periodic flow wave was assigned at the inlet boundary, and a constant pressure was assigned at the outlet. With regard to the bifurcation conditions and the junction conditions between two equivalent tubes, it is assumed that there is no leakage of blood at the bifurcations, the inflow and outflow are balanced, and the pressure is continuous.

The two-step Lax-Wendroff method was employed to compute the blood flow rate and cross-sectional area.

2.2 Darcy model and energy equation for biological tissues

The Darcy model is considered to be the earliest flow transport model in porous media and is expressed as

$$\nabla P = -\frac{\mu}{K} \mathbf{v} \quad (5)$$

where K is the permeability of the tissues, μ is the viscosity, and \mathbf{v} is the Darcy velocity. Based on the assumption that there is a local thermal equilibrium between solid tissues and blood flow, the energy equation is expressed as

$$\begin{aligned} & [(1-\varphi)(\rho c_p)_s + \varphi(\rho c_p)_f] \frac{\partial T_m}{\partial t} + (\rho c_p)_f \mathbf{v} \cdot \nabla T_m \\ & = \nabla \cdot [((1-\varphi)k_s + \varphi k_f) \nabla T_m] + [(1-\varphi)q_s + \varphi q_f] \end{aligned} \quad (6)$$

where

$$(\rho c)_m = \varphi(\rho c)_b + (1-\varphi)(\rho c)_t \quad (7)$$

$$k_m = \varphi k_b + (1-\varphi)k_t \quad (8)$$

$$q_m = \varphi q_b + (1-\varphi)q_t \quad (9)$$

are the overall heat capacity per unit volume, overall thermal conductivity, and overall heat production per unit volume of the tissue, respectively, and φ is the porosity of the tissue.

Considering the continuity equation and momentum equation, the dimensionless pressure in porous media is expressed as

$$\frac{\partial^2 P^*}{\partial x^{*2}} + \frac{\partial^2 P^*}{\partial y^{*2}} = 0 \quad (10)$$

The dimensionless velocity is expressed as

$$u^* = -Da Re \frac{\partial P^*}{\partial x^*} \quad (11)$$

$$v^* = -Da Re \frac{\partial P^*}{\partial y^*} \quad (12)$$

where Da is the Darcy number and is expressed as

$$Da = \frac{K}{D^2} \quad (13)$$

The dimensionless energy equation is as follows:

$$\frac{\partial T^*}{\partial t^*} + \varepsilon \left[u^* \frac{\partial T^*}{\partial x^*} + v^* \frac{\partial T^*}{\partial y^*} \right] = \frac{1}{Pe_m} \left[\frac{\partial^2 T^*}{\partial x^{*2}} + \frac{\partial^2 T^*}{\partial y^{*2}} \right] + \frac{1}{Pe_m} q_m^* \quad (14)$$

where Pe_m , ε , and q_m^* are expressed as follows:

$$Pe_m = \frac{U_\infty D}{\alpha_m} \quad (15)$$

$$\varepsilon = \frac{(\rho c)_b}{(\rho c)_m} \quad (16)$$

$$q_m^* = \frac{q_m D^2}{(T_a - T_\infty) k_m} \quad (17)$$

Equation 14 can be suitably applied for heat transport in both large vessels and tissues. When it is applied to the heat transport in large vessels, both ε and ϕ attain a value of 1.

Equations (10)–(12) and (14) have been discretized using the finite element method (FEM), and the finite element equation has been developed using the Galerkin weighted residual method. First, the conjugate gradient (CG) method was employed to solve the equation (10). The value of the pressure in the large vessels was obtained from the blood flow model and was assigned as the boundary condition of Equation (10). Second, the blood flow velocities in the tissues were computed. The slip condition was employed at the large vessel wall. Finally, the temperatures in large vessels and tissues were computed simultaneously. A constant blood temperature condition was assigned to an inlet of a large artery in the finger. The heat transfer at the skin surface is due to heat convection, radiation, and evaporation. Thus, the boundary condition at the surface can be expressed as

$$-\frac{\partial T}{\partial n} \Big|_\Gamma = BiT \Big|_\Gamma + \frac{h_{ra} D}{\lambda_s} T \Big|_\Gamma + E_{sk} \quad (18)$$

The flowchart of the computational method is shown in Fig. 1.

2.3 Geometrical modelling for the blood vessels and human finger

Since we use a one-dimensional flow model to describe the blood flow in arteries and veins, the data of the

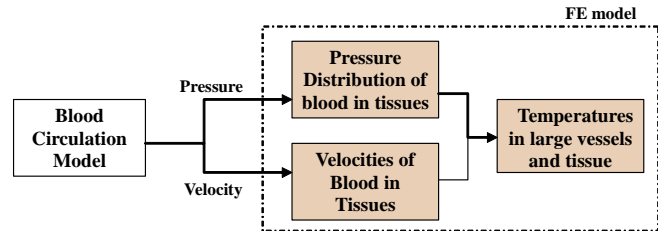


Fig. 1 Flow chart of the computational method

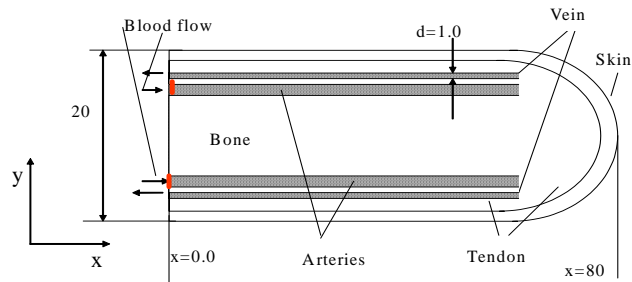


Fig. 2 The schematic diagrams of a finger section in longitudinal direction

cross-sectional area and the length of the blood vessel are required and are defined on the basis of the statistical data [15].

Two types of geometrical models were employed. Of these, one was the finger model for the lateral section and the other was the MR image-based finger model for the vertical section. The dimension of the finger model for the lateral section was determined by the measurement and anatomical data [16, 17] (Fig. 2). The arterial blood flows into the arteries from the base and it flows out from the veins. The number of vessels in the fingertip is large, and it is difficult to describe the blood flow through each vessel. Therefore, the fingertip part is described as a porous media with higher porosity. The finite element meshes were thus developed according to this model.

Fig. 3 shows the process for constructing the finite element model from MR images. The MR images of the vertical section of the human finger and the blood vessels were first taken. The image size was 128×128 (Fig. 3a). Subsequently, several image processing operators were applied in turns to reduce the noise present in the original image and subtract the image data from the background. The image processing includes smoothing, enhancing contrast, and arithmetic subtracting. A processed image was thus obtained (Fig.3b) and a text file with information on the brightness of each pixel in the image was created. The text file of the image information was then inputted and the coordinate of each pixel for the finger was identified and the original finite element model was constructed (Fig. 3c). In order to generate a finite element model for thermofluid computation, the surface of the original model requires smoothing. The smoothing approach is to fit discrete surface areas by linear interpolation and generate meshes over these areas. After surface smoothing, the mesh sizes were regulated such that the meshes around the boundary part were smaller and those in the inner part were coarse.

The MR image of a large artery in the human finger is shown in Fig. 3d. We considered the blood vessels with a diameter smaller than that of the large artery to be the fluid phase in the porous tissue. The position of the pixel expressing blood was identified and the

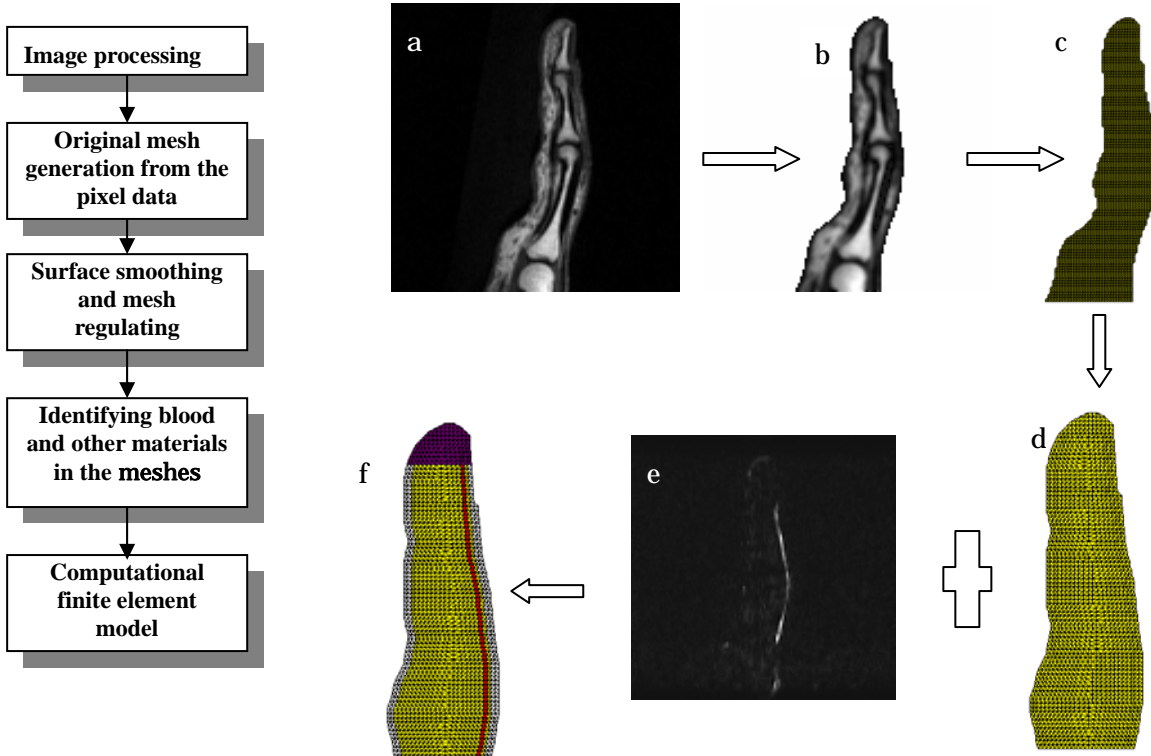


Fig. 3 The process to construct finite element model from MR images

information was added to the element model. Thus, the blood vessel part was classified from the other parts. The fingertip part and the bone part were identified according to the characteristic points in the original MR image. The finite element model for the computation is shown in Fig. 3e in which different materials have been expressed in different colors.

3. Computation results

The thermophysical properties have been listed in Table 1, which are referred to the references [6,18]. It is considered that the porosity of the tissue does not normally exceed 0.6 [19]. Based on the data in [18], we defined the porosity in the bone, tendon, skin, and fingertip as 0, 0.1, 0.2, 0.3, respectively. Due to the large density of the vessels in the fingertip, the porosity was assigned a larger value. Tissue permeability was defined as 10^{-13} m^2 [19]. Fig. 4 shows the variation of pressure in the large arteries and veins in the finger; this is computed by the one-dimensional blood flow model. It can be observed that the pressure difference is greater in the artery, whereas there is only a slight difference in the vein. These data were assigned to the nodes that represent the artery and vein in the finite element model and the pressure was set such that it varied along the blood flow direction but did not change in the direction normal to the flow direction.

The computed inflow velocities in the finger artery and vein are 19 cm/s and 3.5 cm/s, respectively, and the Reynolds number in the computation is 50 when the arterial velocity is the reference velocity. Since the computed velocity along the flow direction slightly changes in the large vessels, it is assigned to the blood nodes with uniform values.

Figs. 5 (a) and (b) show the computed capillary pressure and flow distribution in the lateral section of the finger. It can be observed that the pressure difference is obvious in the fingertip and the blood flow (Fig. 5(b)) is greater than that in other areas. The flow pattern in the tissue is in agreement with the anatomical vasculature (Fig. 5(c)).

Fig. 6(a) shows the temperature distribution in the large vessels and tissues in the lateral section of the finger when the environmental air temperature is 22 °C. It can be observed that the blood temperature in the arteries was relatively higher and the tissue temperature

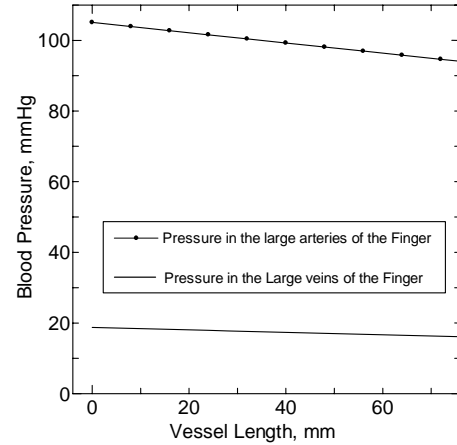
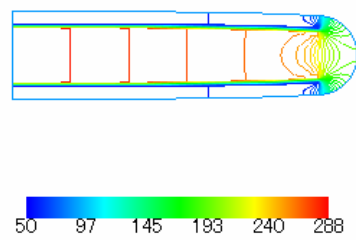


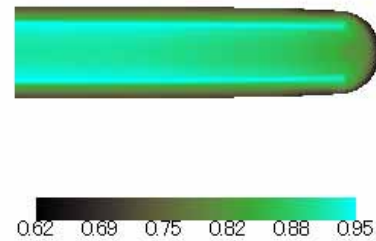
Fig. 4 Pressure distribution in the axial direction of the blood flow in large arteries and veins of the finger

Table 1. Physical properties and porosities

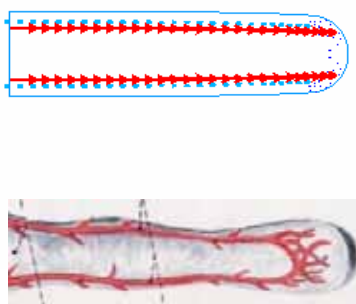
	Bone	Tendon	Skin	Fingertip	Blood
ρ (kg/m ³)	1418	1270	1200	1270	1100
c (J/kgK)	2094	3768	3391	3768	3300
λ (W/mK)	2.21	0.35	0.37	0.35	0.50
q_{meta} (W/m ³)	170	632	250	632	
ϕ	0.0	0.1	0.2	0.3	1.0



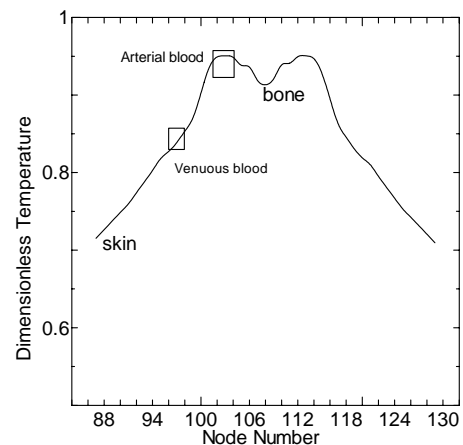
a



a



b



b

Fig. 5 The dimensionless (a) pressure distribution and (b) velocity distribution of blood flow in large vessels and tissues. (c) Anatomical structure of the arteries in the finger [19]

Fig. 6(a) Temperature distribution in the large vessels and tissues of the finger. Fig. 6(b) Temperature profile in a cross section

gradually decreased from the base to the fingertip; this corresponded with the measurement performed by thermography [20]. The temperature profile in a cross section is plotted in Fig. 6 (b). The temperatures indicated by the rectangular marks are blood temperatures. It can be observed that the venous blood temperature is not markedly higher than that of the surrounding tissue as compared to the arterial blood temperature; this implies that the effect of convection in the venous vessel is not as large as that in the arterial vessel.

The computed results using the image-based model are shown in Fig. 7(a) to (c). As shown in Fig. 5(a), an obvious pressure difference existed in the fingertip. Fig. 7(b) reveals that there was considerable blood flow in the tissue of the palm side; this is qualitatively in agreement with the measurement [21] in which the blood perfusion in the palm side of the finger generally ranged from 20 to 70 ml/min/100 g and was considerably lesser in the back of the finger. The temperature distribution when a constant temperature was assigned to the boundary surface in the image-based model is shown in Fig.7 (c). A distribution similar to that in Fig. 6 (a) was obtained.

4. Discussion and conclusions

In this study, we divided the blood flow in the tissues into two groups: one is the blood flow in the large vessels (the diameter of the vessels is generally larger than or equal to 1 mm)

and the other is the blood flow in the microvessels. We used a one-dimensional flow model in an elastic tube to describe the blood flow in the large vessels, and the Darcy model to model the flow in porous media to describe the blood flow in microvessels. The unified energy equation was used to model the heat transfer in larger vessels and in the tissue that was considered as porous media. The initial computed results have shown that the simulated blood flow through tissues is qualitatively in agreement with the anatomical structure and measurement. Since the information on the local blood flow has been obtained from the one-dimensional flow and Darcy models, the thermal effect of different vessels can be evaluated through the energy equation without other parameters.

Another characteristic of this study is that the image-based modeling method was employed to construct the finite element model. The realistic geometry of the finger can be constructed from medical images, and this model can be applied in analyzing other heat transfer problems in other living tissues.

Further, the computational time can be significantly shortened as compared to that using a thorough two-dimensional model [18] to express the blood flow in living tissues.

The limitation of this method is that it requires the conversion of the one-dimensional blood velocity into the two-dimensional information in the finite element model.

In summary, the method based on the one-dimensional flow and the porous media transport model gives favorable results in analyzing heat transfer problems in living tissues. It is believed that by applying the image-based modeling method, more practical applications in personal health care and clinical therapies can be explored.

References

- [1] Pennes, H. H., 1948, Analysis of tissue and arterial blood temperatures in the resting human forearm, *J. Appl. Physiol.*, 1(2), pp. 93-122.
- [2] Keller, K.H. and Seiler, L., 1971, An analysis of peripheral heat transfer in man. *J. Appl. Physiol.* 30(5), pp.779-786.
- [3] Wissler, E. H., 1964, A mathematical model of the human thermal system, *Bulletin of mathematical biophysics*, 26, pp.147-166.
- [4] Charny, C. K. and Levin, R. L., 1991, A three-dimensional thermal and electromagnetic model of whole limb heating with a MAPA, *IEEE transactions on biomedical engineering*, 38 (10), pp.1030-1037.
- [5] Takemori, T., Nakajima, T., and Shoji, Y., 1995, A fundamental model of the human

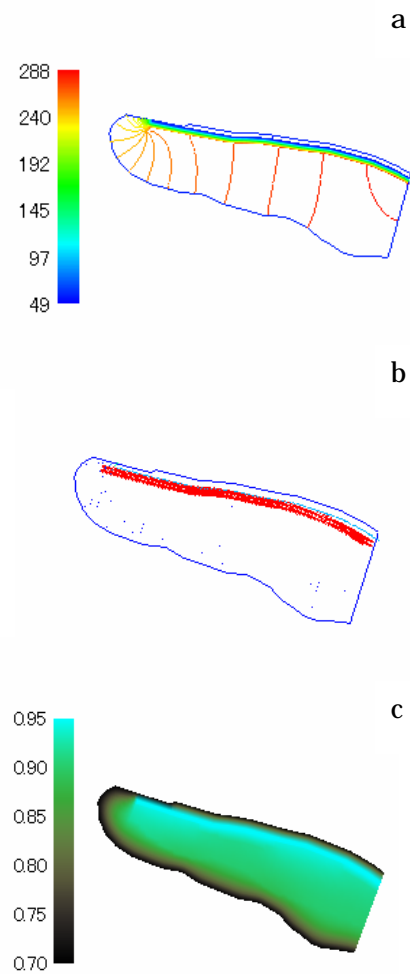


Fig. 7 The computed capillary pressure (a), velocity (b), and temperature(c) in the image-based model of the human finger

- thermal system for prediction of thermal comfort, *Tans. JSME (B)*, 61 (584), pp. 297-304.
- [6] Shitzer, A. Stroschein, L., Vital, A. P. Gonzalez, R. R. and Pandolf, K. B., 1997, Numerical Analysis of an extremity in a cold environment including countercurrent arterio-venous heat exchange, *Trans. ASME, J. biomech. Eng.*, 119, pp. 179-186.
- [7] He, Y., Liu, H., Himeno, R. and Shirazaki, M., 2005, Numerical and experimental study on the relationship between blood circulation and peripheral temperature, *J. mechanics in medicine and biology*. 5(1), pp. 39-53.
- [8] Chen, M. M. and Homles, K. R., 1980, Microvascular contributions in tissue heat transfer, *Annals of the New York Academy of Sciences*, 335, pp.137-150.
- [9] Weibaum, S. and Jiji, L. M., 1985, A new simplified bioheat equation for the effect of blood flow on local average tissue temperature. *J. Biomech. Eng.* 107, pp.131-139.
- [10] Brinck, H. and Werner, J., 1994, Estimation of the thermal effect of blood flow in a branching countercurrent network using a three-dimensional vascular model, *Trans. ASME, J. biomech. Eng.*, 164, pp.324-330.
- [11] Wulff, W., 1974, The energy conservation equation for living tissue, *IEEE transactions on biomedical engineering*, pp.494-495.
- [12] Xuan, Y. M. and Roetzel, W., 1997, Bioequation of the human thermal system, *Chem. Eng. Technol.* 20, pp. 269-276.
- [13] Image-based biomechanics, 2004, *Trans. JSME (A)*, Special issue, 70(697) (Japanese).
- [14] Cebal, J. R. and Löhner, R., 2001, From medical images to anatomically accurate finite element grids, *Int. J. Numer. Meth. Eng.*, 51, pp.985-1008.
- [15] Sheng, C., Sarwal, S. N., Watts, K. C. and Marble, A. E., 1995, Computational Simulation of Blood Flow in Human Systemic Circulation Incorporating an External Force Field, *Medical & Biological Engineering & Computing* 33, pp. 8-17.
- [16] Buchholz, B. and Armstrong, T. J., 1991, An ellipsoidal representation of human hand anthropometry, *Human factors*, 33(4), pp.429-441.
- [17] Kahle, W., Leonhardt, H., Platzer, W., 2000, *Taschenatlas der Anatomie* (Japanese, translated by J. Ochi) Bunkodao, Tokyo.
- [18] Shih, T. C., Kou, H. S. and Lin, W. L., 2003, The Impact of Thermally Significant Blood Vessels in Perfused Tumor Tissue on Thermal Dose Distributions During Thermal Therapies, *Int. Comm. Heat Mass Transfer* 30(7) , pp.975-985.
- [19] Nield, D. A. and Behan, A., 1998, *Convection in Porous Media*, 2nd edition, Springer.
- [20] He, Y., Shirazaki, M. and Himeno, R., 2003, A finite element model for determining the effects of blood flow on the finger temperature distribution, *Proc. of the 6th ASME-JSME thermal jointconference*, Hawaii, TED-AJ03-166.
- [21] He, Y., and Himeno, R., 2005, Investigation of the relationship between peripheral temperature and blood flow of human hands after water heating, *Proc. of thermal engineering conference'05*, Nov., pp. 27-28.